Electronic Supplementary Material (ESI) for Physical Chemistry Chemical Physics

Detection of non-absorbing charge dynamics via refractive index change in dye-sensitized solar cells

Shota Kuwahara, Hiroaki Hata, Soichiro Taya, Naotaka Maeda, Qing Shen, Taro Toyoda and Kenji Katayama

Electronic Supplementary Information (ESI):

The principle of the heterodyne transient grating method (Fig. S1)

When a pump beam is incident on a transmission grating; an intensity pattern of an optical fringe is formed close to the grating. When a sample is placed near the transmission grating, it can be excited by the fringe pattern of the pump light. The refractive index of the liquid changes giving the same pattern as the optical fringe because of photochemical or photothermal processes; the pattern of refractive index change is called a transient grating. When another light beam (probe light) is incident on the transient grating, a part of the probe is transmitted (reference), or another part of the probe is once diffracted by the transmission grating and refracted by the transient grating into the same direction with the reference (signal). The intensity of the mixture of the signal and reference (heterodyne signal) was monitored as the time passed. When the transient grating is composed of an intermediate chemical species, the fringe pattern is gradually lost not only by the intrinsic lifetime of the species but also by the diffusion in the perpendicular direction to the fringe. We can recognize the signal decay was due to lifetime or diffusion by checking the dependence on the grating spacing because the decay time due to the diffusion process depends on it.

TA responses of DSSC monitored at 635 nm and 785 nm (Fig. S2)

The TA responses of DSSC monitored at 635 nm 785 nm were shown in Fig. S2. The data was obtained with the electrolyte of 0.03 M I_2 and 0.3 M LiI in acetonitrile. After measuring the TA response at 635 nm, the light source was changed to 785 nm, and the TA data was obtained. Around 10^{-6} to 10^{-4} s, absorption increase was not observed in the TA response at 785 nm, unlike the response at 635 nm. The absorption increase < 10^{-6} s was larger at 785 nm compared with that at 635 nm, because I_2^- has larger absorption at 785 nm.

TG responses of DSSC monitored at 635 nm and 785 nm (Fig. S3)

The TG responses of DSSC monitored at 635 and 785 nm were shown in Fig. S3. The

experimental conditions were same as the TA measurements mentioned above. The relative intensity of the first TG component in the time range < 10^{-6} s at 785 nm was higher than that at 635 nm probe light. I_2^- and dye cation have stronger absorption at 785 nm, the TG signal in < 10^{-6} s was higher at 785 nm compared with that at 635 nm due to the same reason for the TA responses.

The responses around the fourth TG component were shown in Fig. S3 (b). When the TG response of DSSCs were monitored at 785 nm, the fourth TG component corresponding to the electron/electrolyte recombination and the following diffusion process of redox species showed the same responses as that monitored at 635 nm. Since there is no absorption for the redox species, I_3^-, at 785 nm wavelength (Fig. S3 (c)). Thus, the TG responses were not caused by the absorption change due to decrease in I_3^- concentration.

TG responses of DSSC under short circuit condition and open circuit condition (Fig. S4)

The TG responses of a DSSC were monitored at 635 nm probe light. The comparison of TG responses under short circuit condition and open circuit condition were shown in Fig. S4. We performed a two electrode measurement, and the external bias was applied by using a potentiostat. The open circuit voltage (V_{OC} = -0.6 V) was determined as the photocurrent induced by the probe light with a constant intensity was set to zero, and the photocurrent was remained to be zero in the the measurements under open circuit condition.

TA responses of DSSC (Fig. S5)

The comparison of the TA responses for different solvents with different viscosities was shown in Fig. S5. ACN and MPN including the same redox species and additives were used for electrolytes in this study. The TA responses of DSSC were monitored at 635 nm. The decay of the third component was caused by the difference of the redox accessibility to the electrode due to the viscosity change.

TG and TA responses of DSSC in low redox couple concentration (Fig. S6)

The comparison of the TA and the TG responses of DSSCs were shown in Fig. S6. The redox concentration was 3 mM I_2 and 30 mM LiI. Under this condition, the fourth TG component and the third TA component showed an apparent difference on their time constants. This means that TG observes different carrier dynamics with the one TA observed.

(a)

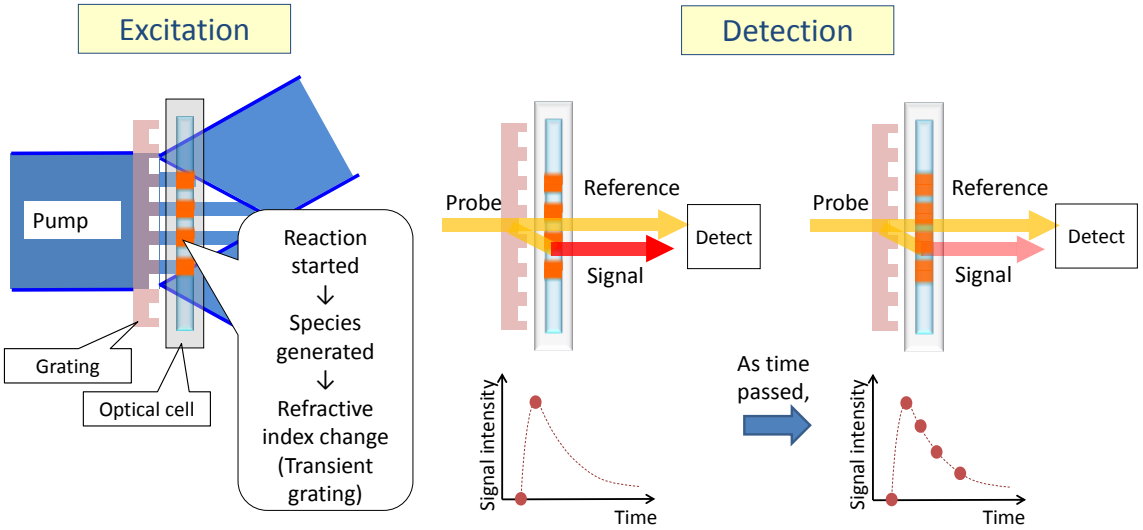

(b)

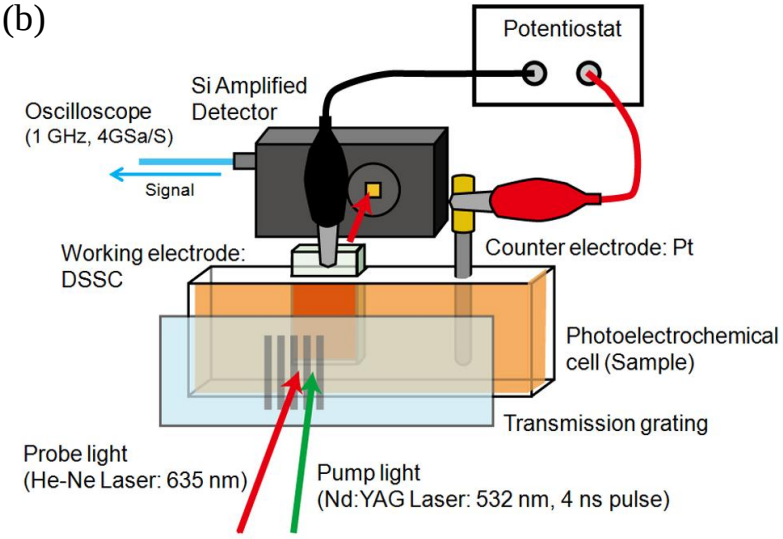

Fig.S1 (a) Schematic diagram of the heterodyne transient grating method and (b) the experimental setup for this work.

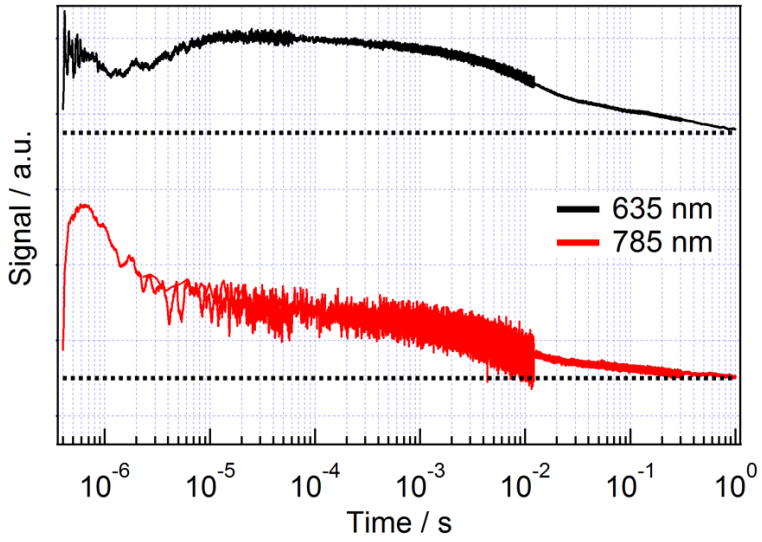

Fig. S2 TA responses of DSSC monitored at 635 nm and 785 nm respectively.

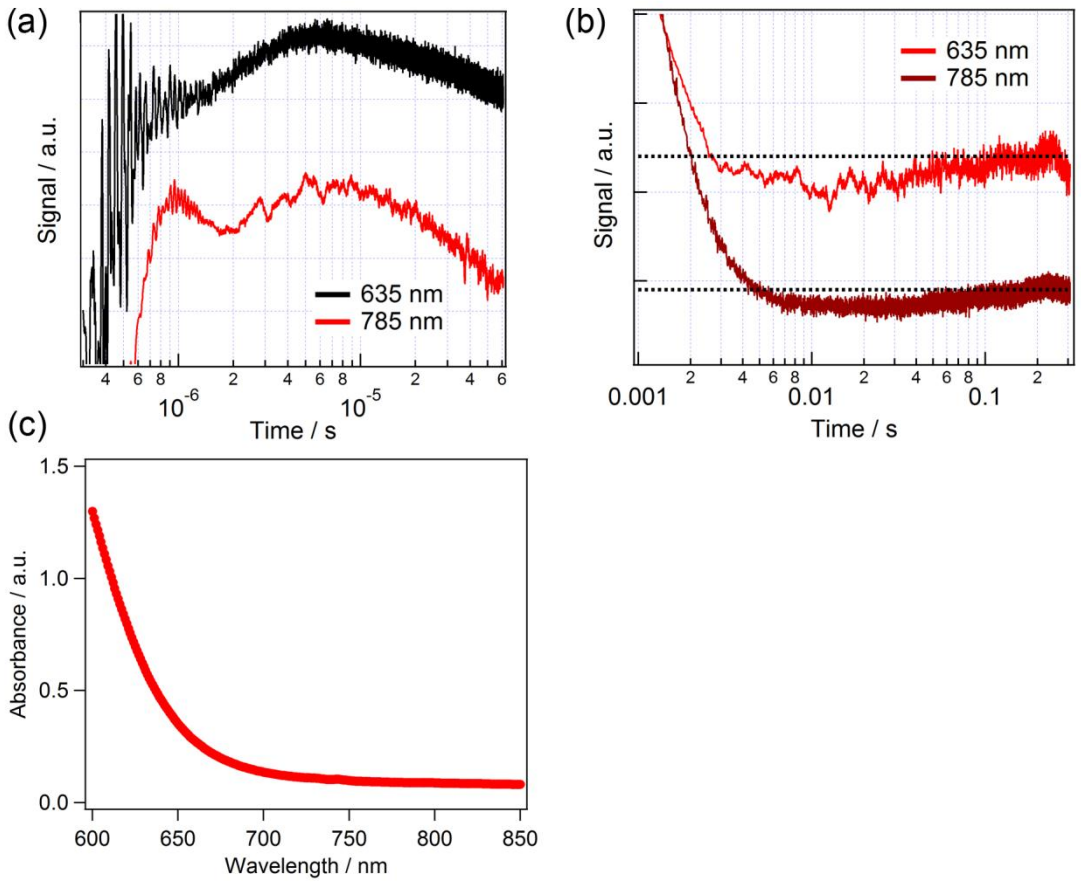

Fig. S3 TG responses of DSSC in the time region (a) < 10^{-4} s, and (b) 10^{-3} to 0.3 s monitored at 635 nm and 785 nm. The absorption spectrum of the used redox (0.03 M I_2 and 0.3 M LiI) in acetonitrile was shown in (c).

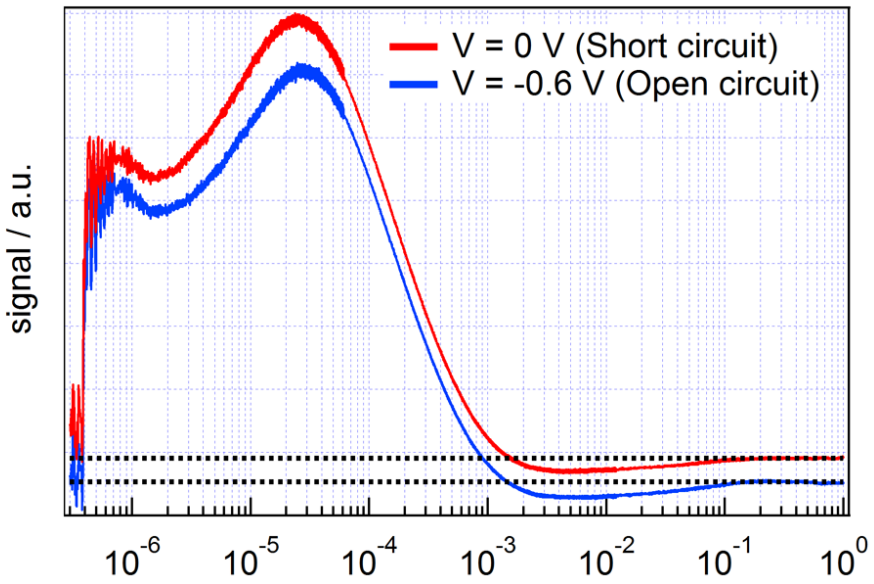

Fig. S4 TG responses of DSSC monitored at 635 nm under short circuit condition and open circuit condition respectively. Each horizontal black dashed line shows the background of the signal.

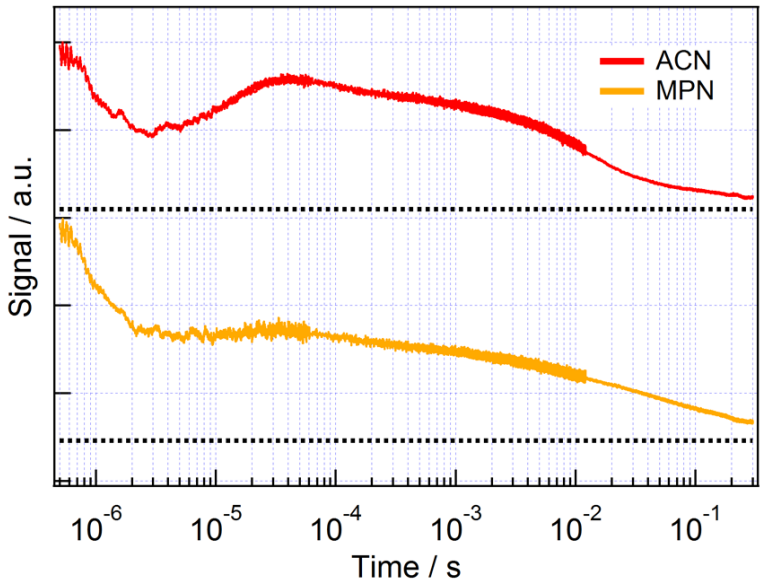

Fig. S5 TA responses of DSSC monitored at 635 nm in ACN and MPN. The horizontal black dashed line shows the background of the signal.

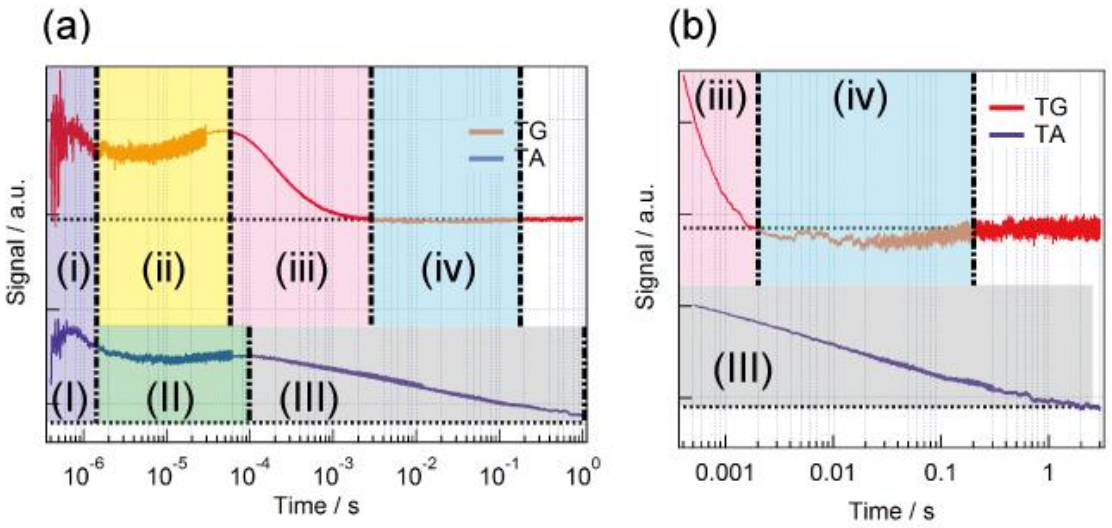

Fig. S6 (a) TA and TG responses of DSSC for a lower redox concentration, whose concentration corresponds to the dilution rate of 0.1 of the one used in Fig. 3. (b) is the enlarged figure of (a) in the time region is 4 x 10^{-4} s to 3 s. Each component was categorized in both the figures. The horizontal black dashed line shows the background of the signals. The TA response was monitored at 635 nm. The horizontal axis is plotted on a logarithmic scale.